SPECIFICS OF THERMOPHYSICAL PROPERTIES AND HEAT TRANSFER AT SUPERCRITICAL PRESSURES

Pioro* I., Sidawi Kh. and Abdullah R.
*Author for correspondence
Faculty of Energy Systems and Nuclear Science
University of Ontario Institute of Technology
2000 Simcoe Street North
Oshawa, Ontario L1H 7K4
Canada
E-mail: igor.pioro@uoit.ca

ABSTRACT

Currently, SuperCritical Fluids (SFCs) are used in various industries worldwide. The largest application of SCFs is the use of SuperCritical Water (SCW) at SuperCritical Pressure (SCP) coal-fired power plants. Using SCP Rankine "steam" cycle allows to reach gross thermal efficiencies of a plant up to 55%. On contrary, current subcritical-pressure water-cooled Nuclear Power Plants (NPPs) of Generations II and III have significantly lower gross thermal efficiencies within the range of 30 - 36% (up to 37 - 38% for Generation III$^+$ nuclear-power reactors).

To increase efficiency of next generation – Generation IV NPPs higher parameters (mainly temperature) should be reached for reactors' coolants and corresponding to that for power cycles. Analysis of Generation IV nuclear-reactor concepts shows that three concepts will be cooled with SCFs such as helium and water, and there is a possibility that other concepts will be linked to SCP Rankine cycle or to SCP Brayton cycle with helium or carbon dioxide working fluids.

Therefore, specifics of thermophysical properties and heat transfer of SCFs are very important for reliability and safety of new thermal and nuclear power plants. Also, for SCW nuclear reactors heat transfer to SCW flowing inside various bundle geometries has to be understood and estimated.

INTRODUCTION

The use of SuperCritical Fluids (SCFs) in different processes is not new, and nor was it a human invention. Mother Nature has been processing minerals in aqueous solutions at near or above the critical point of water for billions of years (Levelt Sengers, 2000). It was only in the late 1800's when scientists started to use this natural process, called hydrothermal processing, in their labs for creating various crystals. During the last 50 – 60 years, this process (operating parameters - water pressures from 20 to 200 MPa and temperatures from 300 to 500ºC) has been widely used in the industrial production of high-quality single crystals (mainly gem stones).

First works devoted to the problem of Heat Transfer (HT) at SuperCritical Pressures (SCPs) started as early as the 1930s. Schmidt et al. (1946) investigated free-convection HT of fluids at the near-critical point with the application to a new effective cooling system for turbine blades in jet engines.

In the 1950s, the idea of using SuperCritical Water (SCW) appeared to be rather attractive for steam generators/turbines in the thermal-power industry. The objective was to increase the total thermal efficiency of coal-fired power plants (Pioro and Duffey, 2007). At SCPs there is no liquid-vapour phase transition; therefore, there is no such phenomenon as critical heat flux or dryout. It is only within a certain range of parameters that deteriorated HT may occur. Therefore, the objective of this paper is a discussion on specifics of thermophysical properties and HT of SCFs in power-engineering applications.

NOMENCLATURE

c_p	specific heat at constant pressure, J/kg K
$\overline{c}_p$	average specific heat, J/kg·K $\left(\frac{H_w - H_b}{T_w - T_b}\right)$
D	inside diameter, m
G	mass flux, kg/m^{2}s
H	specific enthalpy, J/kg
h	heat transfer coefficient, W/m^{2}K
k	thermal conductivity, W/m K
P, p	pressure, MPa
Q	heat-transfer rate, W
q	heat flux, W/m^2
T, t	temperature, ºC
V	specific volume, m^3/kg

Greek Letters

μ	dynamic viscosity, Pa·s
ρ	density, kg/m^3

Non-dimensional Numbers

Nu	Nusselt number; $\left(\frac{h \cdot D}{k}\right)$
Pr	Prandtl number; $\left(\frac{\mu \cdot c_p}{k}\right)$
$\overline{\mathbf{Pr}}$	average Prandtl number, $\left(\frac{\mu \cdot \overline{c_p}}{k}\right)$
Re	Reynolds number; $\left(\frac{G \cdot D}{\mu}\right)$

Subscripts or superscripts

ave average
b bulk
cr critical
in inlet
pc pseudocritical
w wall

Abbreviations and acronyms

DHT Deteriorated Heat Transfer
HT Heat Transfer
HTC Heat Transfer Coefficient
HTR High Temperature Reactor (helium cooled)
ID Inside Diameter
IHT Improved Heat Transfer
LFR Lead-cooled Fast Reactor
NHT Normal Heat Transfer
NPP Nuclear Power Plant
SCF SuperCritical Fluid
SCW SuperCritical Water
SCWR SuperCritical Water-cooled Reactor
SFR Sodium-cooled Fast Reactor

SUPERCRITICAL-PRESSURE THERMAL POWER PLANTS

It is well known that electrical-power generation is the key factor for advances in any other industries, agriculture and level of living. For about 100 years, coal was used for generating electrical energy at coal-fired thermal-power plants worldwide. All coal-fired power plants operate based on, the so-called, steam Rankine cycle, which can be organized at two different levels of pressures: 1) older or smaller capacity power plants operate at steam pressures no higher than 16-17 MPa; and 2) modern large capacity power plants operate at SCPs from 23.5 MPa and up to 38 MPa. Supercritical pressures refer to pressures above the critical pressure of water, which is 22.064 MPa.

From a thermodynamics perspective, it is well known that higher thermal efficiencies correspond to higher temperatures and pressures (see Table 1). Using SCW-"steam" at coal-fired thermal-power plants is the largest application of SCFs in the power industry. However, in spite of advances in coal-fired power-plant, they are still not considered to be environmental friendly due to production of carbon-dioxide emissions, as a result of the combustion process, plus production of ash, slag and even acid rains.

FUTURE APPLICATIONS OF SCFS IN NUCLEAR POWER PLANTS

In general, nuclear power, as coal and other fossil fuels, is a non-renewable resource. However, nuclear resources can be used for a significantly longer period of time when compared to some fossil fuels, plus nuclear power does not emit carbon dioxide into the atmosphere. Currently, this source of energy is considered the most viable option of electrical generation for the next 50 – 100 years (Pioro and Duffey, 2015).

Current nuclear reactors, i.e., Generation II and III, consist of water-cooled reactor Nuclear Power Plants (NPPs) with a thermal efficiency of 30 – 36% (vast majority of reactors, i.e., 96%); carbon-dioxide-cooled reactor NPPs with a thermal efficiency up to 42% and liquid-sodium-cooled reactor NPPs with a thermal efficiency up to 40% (see Table 2). Within the next 5 – 10 years, Generation III+ (2010 – 2025) reactors with improved parameters (water-cooled NPPs with a thermal efficiency up to 38%) will be implemented. However, these reactors will have only evolutionary design improvements. Therefore, the next generation or Generation IV (2025 - …) reactors with new parameters (NPPs with the thermal efficiency of 43 – 50% and even higher) are currently under development worldwide (see Table 3).

The Generation-IV International Forum (GIF) Program has narrowed design options of nuclear reactors to six concepts (Handbook (2016); Pioro and Kirillov, 2013c). These concepts are:

1) Gas-cooled Fast Reactor (GFR) or just High Temperature Reactor (HTR);
2) Very High Temperature Reactor (VHTR);
3) Sodium-cooled Fast Reactor (SFR);
4) Lead-cooled Fast Reactor (LFR) (see Fig. 1);
5) Molten Salt Reactor (MSR); and
6) SuperCritical Water-cooled Reactor (SCWR) (see Fig. 2)

(IAEA, 2014; Pioro, 2011; Pioro and Duffey, 2007).

Possible applications of SCP technologies in Generation IV nuclear-reactor concepts are as the following:

I. Supercritical Fluids as Reactor Coolants
   1. SCWRs will use SCW (P_{cr}=22.064 MPa and T_{cr}=373.95°C)
   2. Both GFRs (HTRs) and VHTRs will use SC Helium (P_{cr}=0.2276 MPa and T_{cr}=-267.95°C)

II. Supercritical-Pressure Power Cycles
   1. SCWRs with direct or in-direct cycles will use SCP Rankine Cycle;
   2. LFR (Russian design) will use SCP Rankine Cycle;
   3. Both GFRs (HTRs) and VHTRs might use SCP-Helium Brayton Gas-Turbine Cycle (there is a possibility that GFRs (HTRs) will use SCP-Carbon-Dioxide Brayton Gas-Turbine Cycle (P_{cr}=7.3773 MPa and T_{cr}=30.978°C)).
   4. SFRs (USA concept) and MSRs will use SCP-Carbon-Dioxide Brayton Gas-Turbine Cycle.

In addition, the SC carbon-dioxide Brayton gas-turbine cycle is also considered for implementation in Generation IV nuclear-reactor concepts, such as Sodium-cooled Fast Reactors (SFRs), Lead-cooled Fast Reactors (LFRs) (Fig. 1) and High Temperature helium-cooled Reactors (HTRs). Therefore, knowledge of thermophysical-properties and HT specifics at SCPs is very important for efficient use of SCFs in various industries.

Table 1. Typical ranges of thermal efficiencies (gross[1]) of modern thermal power plants (Pioro and Duffey, 2015; Pioro and Kirillov, 2013a).

No	Thermal Power Plant	Eff., %
1	Combined-cycle power plant (combination of Brayton gas-turbine cycle (fuel - natural gas or LNG; combustion-products parameters at the gas-turbine inlet: T_{in}≈1650°C) and Rankine steam-turbine cycle (steam parameters at the turbine inlet: T_{in}≈620°C (T_{cr}=374°C)).	Up to 62
2	Supercritical-pressure coal-fired power plant (Rankine-cycle steam inlet turbine parameters: P_{in}≈25–38 MPa (P_{cr}=22.064 MPa), T_{in}≈540-625°C (T_{cr}=374°C) and T_{reheat}≈540-625°C).	Up to 55
3	Internal-combustion-engine generators (Diesel cycle and Otto cycle with natural gas as a fuel).	Up to 50
4	Subcritical-pressure coal-fired power plant (older plants) (Rankine-cycle steam: P_{in}≈17 MPa, T_{in}≈540°C (T_{cr}=374°C) and T_{reheat}≈540°C).	Up to 40
5	Concentrated-solar thermal power plants with heliostats, solar receiver (heat exchanger) on a tower and molten-salt heat-storage system (for details, see Fig. 9): Molten-salt maximum temperature is about 565°C, Rankine steam-turbine power cycle used.	Up to 20

Table 2. Typical ranges of thermal efficiencies (gross[2]) of modern nuclear power plants (Pioro and Duffey, 2015; Pioro and Kirillov, 2013b). (*T*-*s* diagrams of various power cycles of NPPs are shown in Dragunov et al. (2015) and a comparison of various properties of nuclear-reactor coolants – in Dragunov et al. (2014)).

No	Nuclear Power Plant	Eff., %
3	Carbon-dioxide-cooled reactor NPP (Generation-III) (reactor coolant: P=4 MPa & T=290-650°C; steam: P=17 MPa (T_{sat}=352°C) & T_{in}=560°C)	Up to 42
4	Sodium-cooled fast reactor NPP (Generation-IV) (steam: P=14 MPa (T_{sat}=337°C) & T_{in}=505°C)	Up to 40
6	Pressurized Water Reactor NPP (Generation-III+, to be implemented within next 1-10 years) (reactor coolant: P=15.5 MPa & T_{out}=327°C; steam: P=7.8 MPa & T_{in}=293°C)	Up to 38
7	Pressurized Water Reactor NPP (Generation-III, current fleet) (reactor coolant: P=15.5 MPa & T_{out}=292-329°C; steam: P=6.9 MPa & T_{in}=285°C)	Up to 36
8	Boiling Water Reactor NPP (Generation-III, current fleet) (P_{in}=7.2 MPa & T_{in}=288°C)	Up to 34
9	RBMK (boiling, pressure-channel) (Generation-III, current fleet) (P_{in}=6.6 MPa & T_{in}=282°C)	Up to 32
10	Pressurized Heavy Water Reactor NPP (Generation-III, current fleet) (reactor coolant: P=11 MPa & T=260-310°C; steam: P=4.7 MPa & T_{in}=260°C)	Up to 32-34

Table 3. Estimated ranges of thermal efficiencies (gross) of Generation-IV NPP concepts (shown here just for reference purposes).

No	Nuclear Power Plant	Eff., %
1	Very High Temperature Reactor (VHTR) NPP (reactor coolant – helium: P=7 MPa and T_{in}/T_{out}=640/1000°C; primary power cycle – direct Brayton gas-turbine cycle; possible back-up – indirect Rankine steam cycle).	≥55
2	Gas-cooled Fast Reactor (GFR) or High Temperature Reactor (HTR) NPP (reactor coolant – helium: P=9 MPa and T_{in}/T_{out}=490/850°C; primary power cycle – direct Brayton gas-turbine cycle; possible back-up – indirect Rankine steam cycle).	≥50

[1] Gross thermal efficiency of a unit during a given period of time is the ratio of the gross electrical energy generated by a unit to the thermal energy of a fuel consumed during the same period by the same unit. The difference between gross and net thermal efficiencies includes internal needs for electrical energy of a power plant, which might be not so small (5% or even more).

[2] Gross thermal efficiency of a unit during a given period of time is the ratio of the gross electrical energy generated by a unit to the thermal energy of a fuel consumed during the same period by the same unit. The difference between gross and net thermal efficiencies includes internal needs for electrical energy of a power plant, which might be not so small (5% or even more).

No	Nuclear Power Plant	Eff., %
3	SuperCritical Water-cooled Reactor (SCWR) NPP (one of Canadian concepts; reactor coolant – light water: P=25 MPa and T_{in}/T_{out}=350/625°C (T_{cr}=374°C); direct cycle; high-temperature steam superheat: T_{out}=625°C; possible back-up - indirect supercritical-pressure Rankine steam cycle with high-temperature steam superheat).	45-50
4	Molten Salt Reactor (MSR) NPP (reactor coolant – sodium-fluoride salt with dissolved uranium fuel: T_{out}=700/800°C; primary power cycle – indirect supercritical-pressure carbon-dioxide Brayton gas-turbine cycle; possible back-up – indirect Rankine steam cycle).	~50%
5	Lead-cooled Fast Reactor (LFR) NPP (Russian design Brest-300: reactor coolant – liquid lead: P≈0.1 MPa and T_{in}/T_{out}=420/540°C; primary power cycle – indirect supercritical-pressure Rankine steam cycle: P_{in}≈24.5 MPa (P_{cr}=22.064 MPa) and T_{in}/T_{out}=340/520°C (T_{cr}=374°C); high-temperature steam superheat; possible back-up in some other countries – indirect supercritical-pressure carbon-dioxide Brayton gas-turbine cycle).	~43
6	Sodium-cooled Fast Reactor (SFR) NPP (Russian design BN-600: reactor coolant – liquid sodium (primary circuit): P≈0.1 MPa and T_{in}/T_{out}=380/550°C; liquid sodium (secondary circuit): T_{in}/T_{out}=320/520°C; primary power cycle – indirect Rankine steam cycle: P_{in}≈14.2 MPa (T_{sat}≈337°C) and $T_{in\ max}$=505°C (T_{cr}=374°C); steam superheat: P≈2.45 MPa and T_{in}/T_{out}=246/505°C; possible back-up in some other countries - indirect supercritical-pressure carbon-dioxide Brayton gas-turbine cycle).	~40

DEFINITIONS OF TERMS AND EXPRESSIONS RELATED TO CRITICAL AND SC REGIONS

Prior to a general discussion on specifics of thermophysical properties and forced-convective HT at critical and SCPs, it is important to define special terms and expressions used at these conditions. For a better understanding of these terms and expressions their definitions are listed below together with corresponding Figs. 3 and 4 (for other details, see [4, 7-9]).

Compressed fluid is a fluid at a pressure above the critical pressure, but at a temperature below the critical temperature.
Critical point (also called a *critical state*) is a point in which the distinction between the liquid and gas (or vapour) phases disappears, i.e., both phases have the same temperature, pressure and specific volume or density. The *critical point* is characterized with the phase-state parameters T_{cr}, P_{cr} and V_{cr} (or ρ_{cr}), which have unique values for each pure substance.

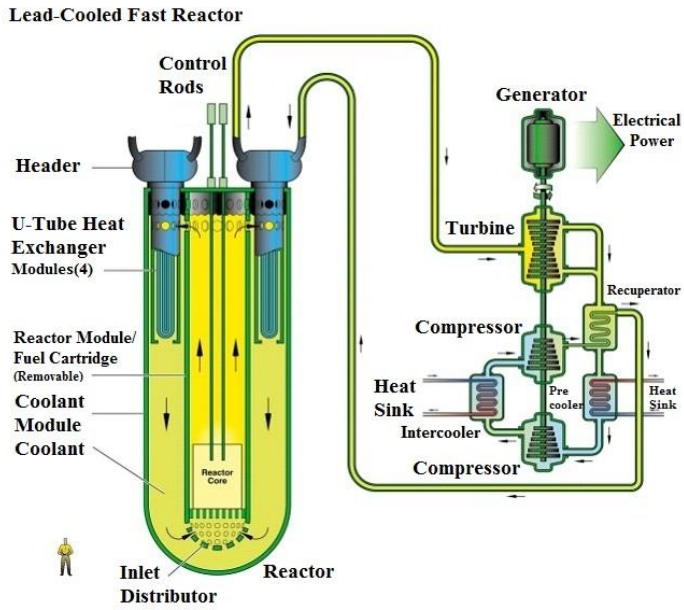

Figure 1. LFR with SC-carbon-dioxide Brayton cycle (courtesy of GIF).

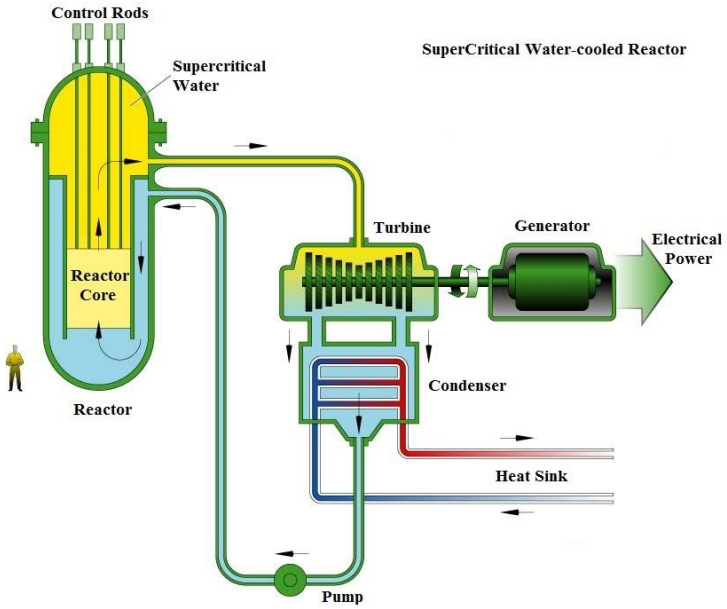

Figure 2. SCWR schematic: US pressure-vessel concept (courtesy of GIF).

Deteriorated Heat Transfer (DHT) is characterized with lower values of the Heat Transfer Coefficient (HTC) compared to those for normal HT; and hence, has higher values of wall temperature within some part of a heated section or within the entire heated section.
Improved Heat Transfer (IHT) is characterized with higher values of the HTC compared to those for normal HT; and hence,

lower values of wall temperature within some part of a heated section or within the entire heated section. In our opinion, the IHT regime includes peaks or "humps" in HTC near the critical or pseudocritical points.

Near-critical point is actually a narrow region around the critical point, where all thermophysical properties of a pure fluid exhibit rapid variations.

Normal Heat Transfer (NHT) can be characterized in general with HTCs similar to those of subcritical convective HT far from critical or pseudocritical regions, when they are calculated according to the conventional single-phase Dittus-Boelter-type correlations: $\mathbf{Nu} = 0.023\ \mathbf{Re}^{0.8}\mathbf{Pr}^{0.4}$.

Pseudocritical line is the line, which consists of pseudocritical points.

Pseudocritical point (characterized with P_{pc} and T_{pc}) is the point at a pressure above the critical pressure and at a temperature ($T_{pc} > T_{cr}$) corresponding to the maximum value of the specific heat at this particular pressure.

SuperCritical Fluid (SCF) is a fluid at pressures and temperatures that are higher than the critical pressure and critical temperature. However, in the present paper, the term "SCF" includes both terms – a *supercritical fluid* and *compressed fluid*.

Supercritical "steam" is actually SCW, because at SCPs fluid is considered as a single-phase substance. However, this term is widely (and incorrectly) used in the literature in relation to SC "steam" generators and turbines.

Superheated vapor (steam) is vapor (steam) at pressures below the critical pressure, but at temperatures above the critical temperature.

Specifics of Thermophysical Properties at Critical and Supercritical Pressures

General trends of various properties near critical and pseudocritical points (Handbook, 2016; Gupta et al. 2013; Pioro et al., 2011; Pioro and Mokry, 2011; Pioro and Duffey, 2007) can be illustrated on a basis of those of water (Figs. 5-8). Properties variations of SC carbon dioxide, helium and R-134a are shown in Pioro and Duffey (2007). Figures 5 through 8 show profiles of basic thermophysical properties of water at the critical (P_{cr} = 22.064 MPa) and three SCPs (P = 25.0, 30.0, and 35.0 MPa), and at three subcritical pressures (P = 7.0, 11.0, and 15.0 MPa) for comparison purposes.

At critical and supercritical pressures a fluid is considered as a single-phase substance in spite of the fact that all thermophysical properties undergo significant changes within the critical and pseudocritical regions. Near the critical point these changes are dramatic. In the vicinity of pseudocritical points with an increase in pressure these changes become less pronounced (see Figs. 5-8).

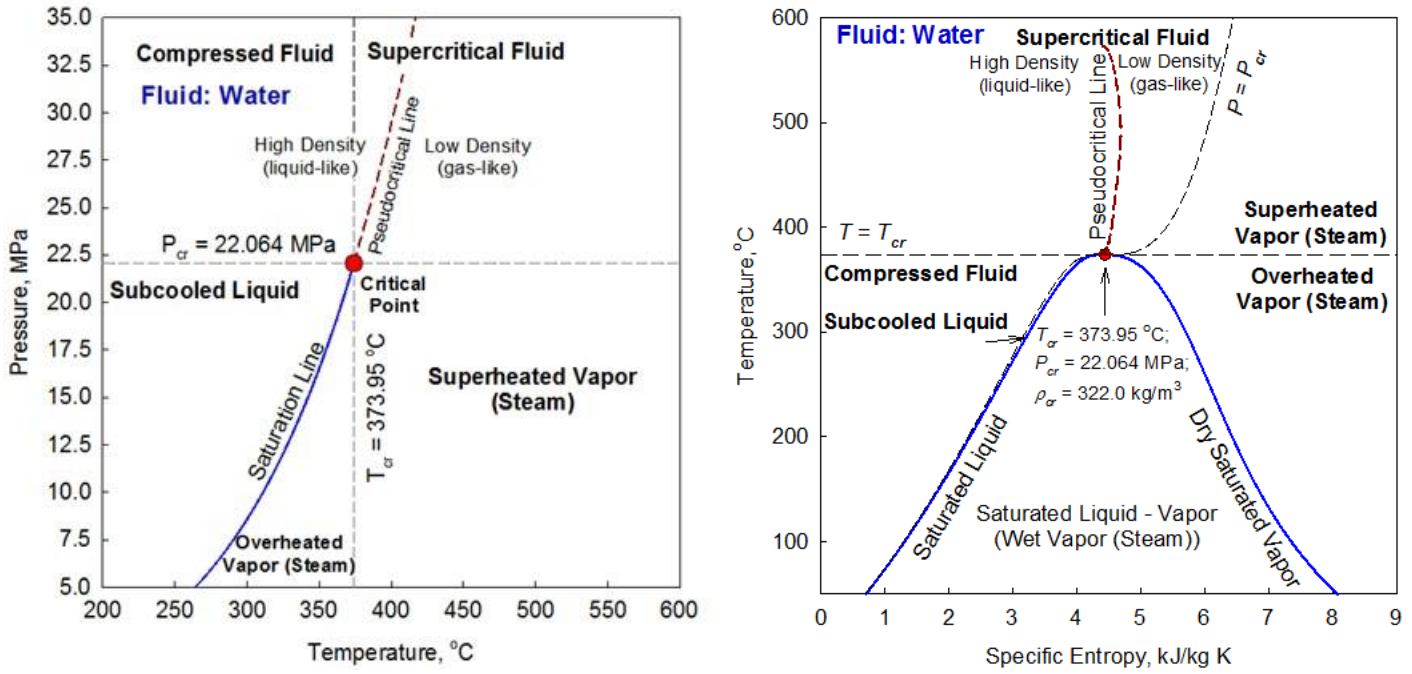

(a) **(b)**

Figure 3. Thermodynamics diagrams for water: (a) Pressure – Temperature and (b) Temperature – Specific Entropy (based on data from NIST (2010).

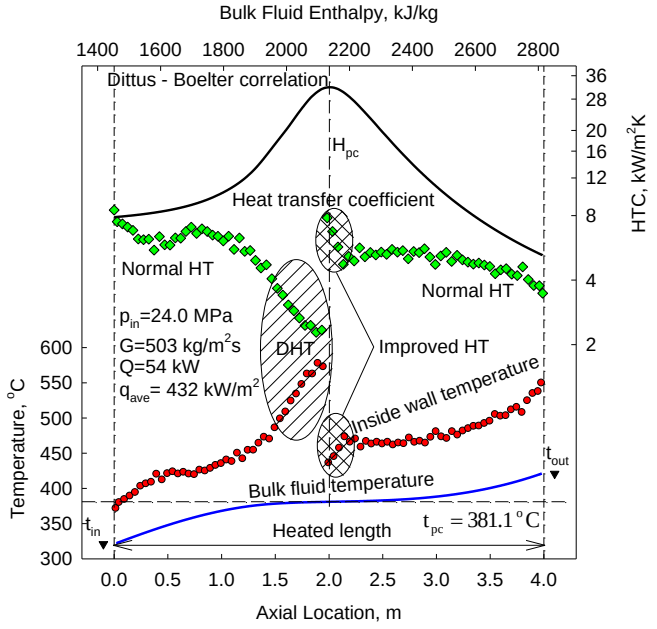

Figure 4. Temperature and HTC profiles along heated length of vertical circular tube (ID 10 mm) with upward flow of SCW (Mokry et al., 2011).

Also, it can be seen that properties such as density and dynamic viscosity undergo a significant drop (near the critical point this drop is almost vertical) within a very narrow temperature range (see Figs. 5a and 6a, respectively), while the kinematic viscosity and specific enthalpy undergo a sharp increase (for details, see Pioro and Duffey (2007)). The volume expansivity, specific heat (see Fig. 7a), thermal conductivity (see Fig. 8a) and Prandtl number have peaks near the critical and pseudocritical points. The magnitude of these peaks decreases very quickly with an increase in pressure. Also, "peaks" transform into "humps" profiles at pressures beyond the critical pressure. It should be noted that the dynamic viscosity (Fig. 6a), kinematic viscosity and thermal conductivity (Fig. 8a) undergo through their minimum right after the critical and pseudocritical points.

Therefore, these effects should be accounted for in HT correlations for SCFs. Usually, these effects accounted for through the cross-section average specific heat ($\bar{c}_p$) and corresponding to that the average Prandtl number ($\overline{\mathbf{Pr}}$), and extra non-dimensional terms (mainly, ratios of various properties obtained at bulk and wall temperatures). The rest of the properties in Nusselt and Reynolds numbers should be evaluated at the characteristic temperature.

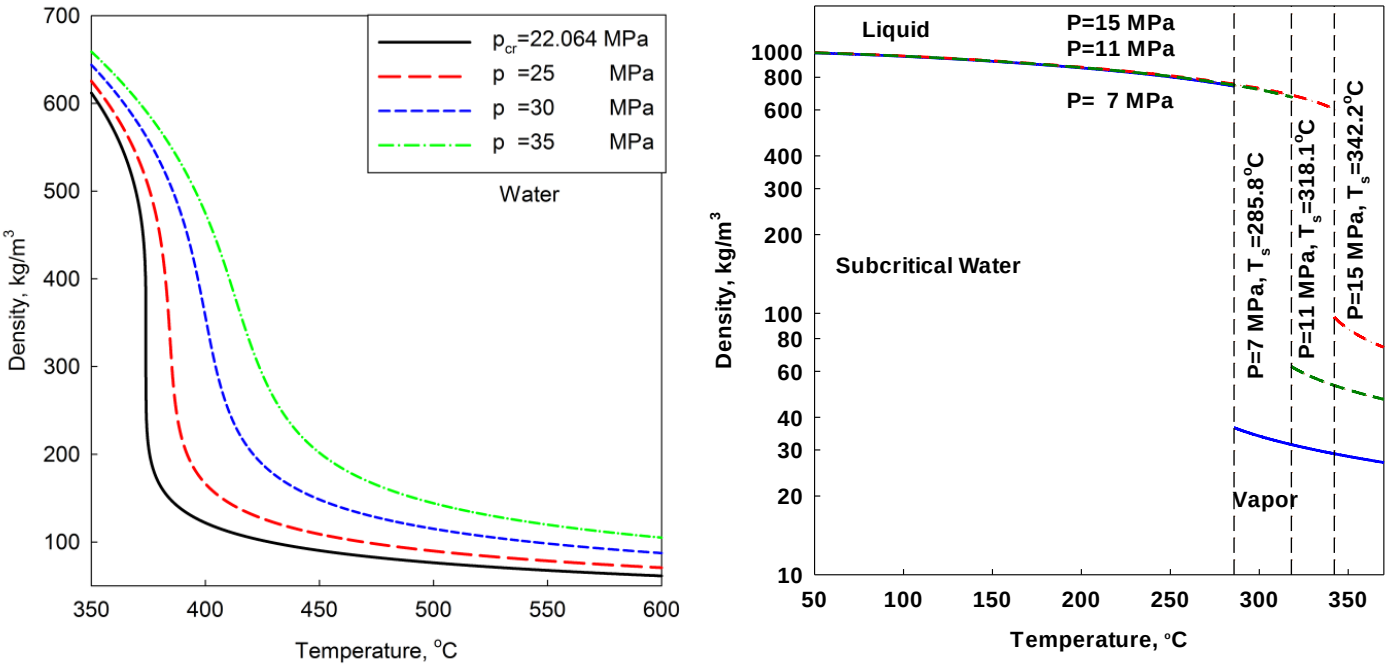

(a) **(b)**

Figure 5. Density vs. Temperature: Water (a) Critical and supercritical pressures and (b) subcritical pressures.

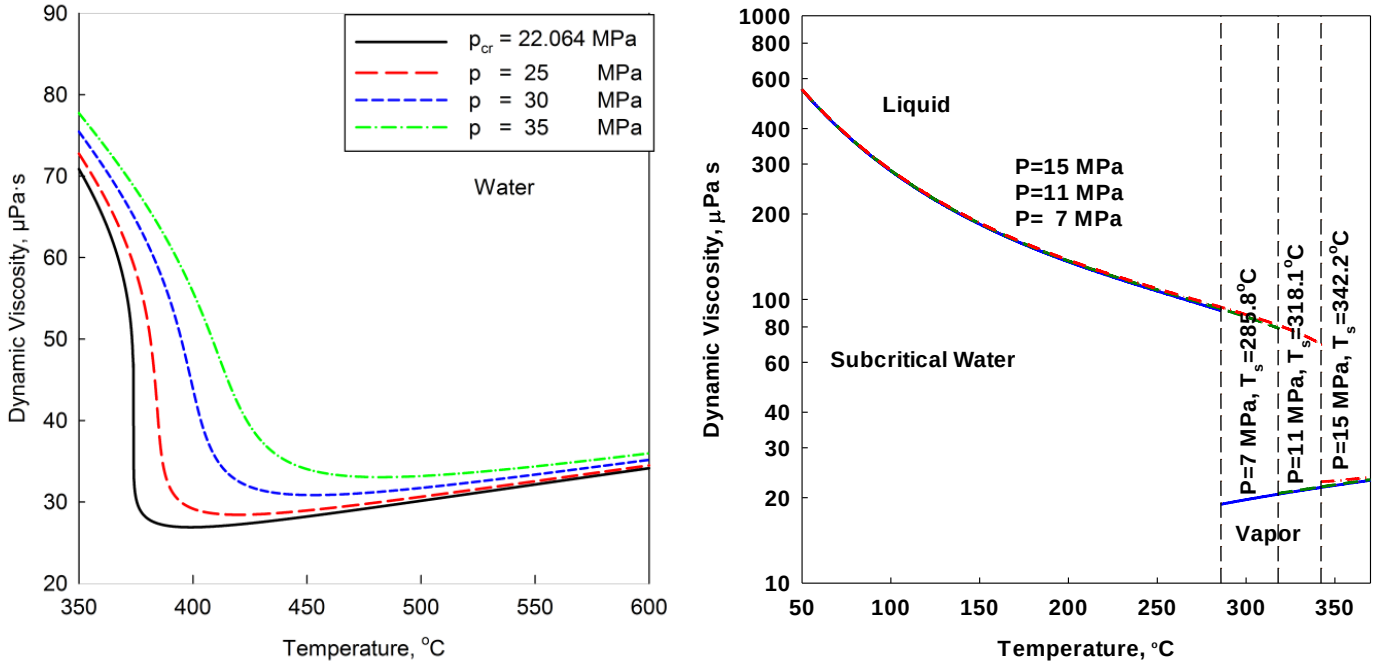

(a) **(b)**

Figure 6a. Dynamic viscosity vs. Temperature: Water (a) Critical and supercritical pressures and (b) subcritical pressures.

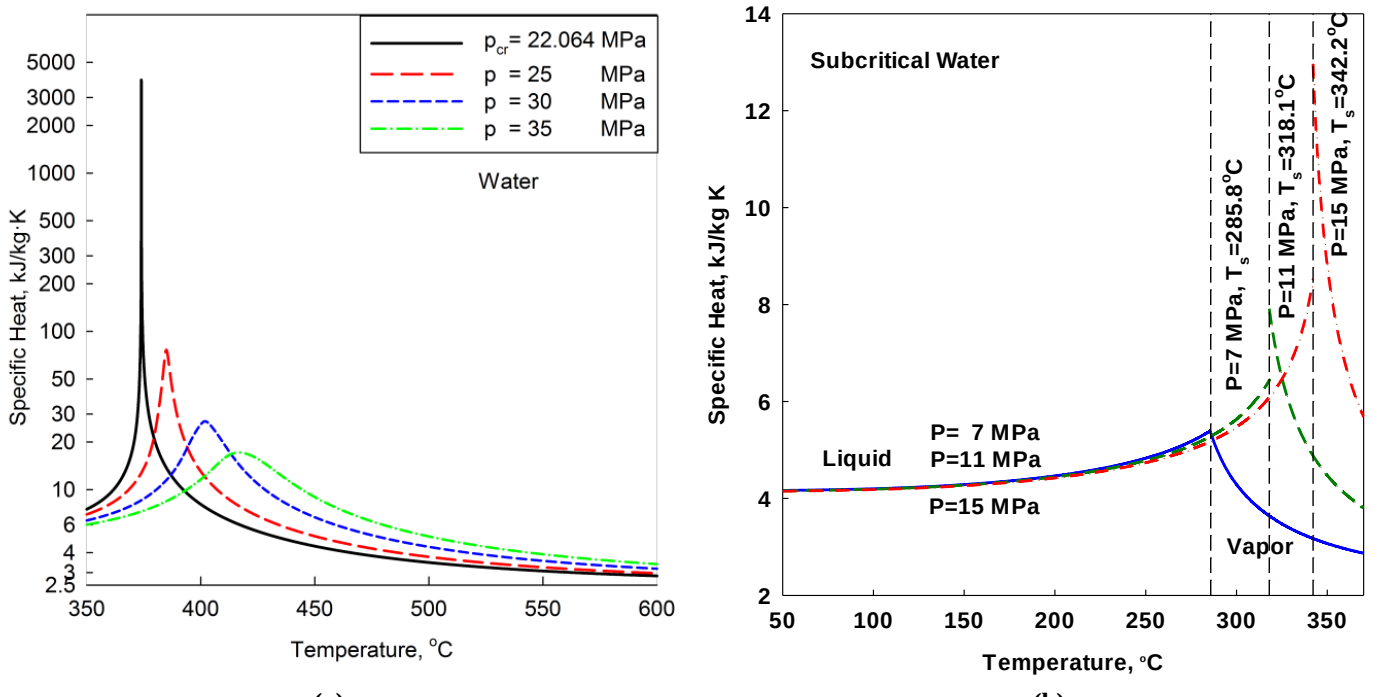

(a) **(b)**

Figure 7a. Specific heat vs. Temperature: Water (a) Critical and supercritical pressures and (b) subcritical pressures.

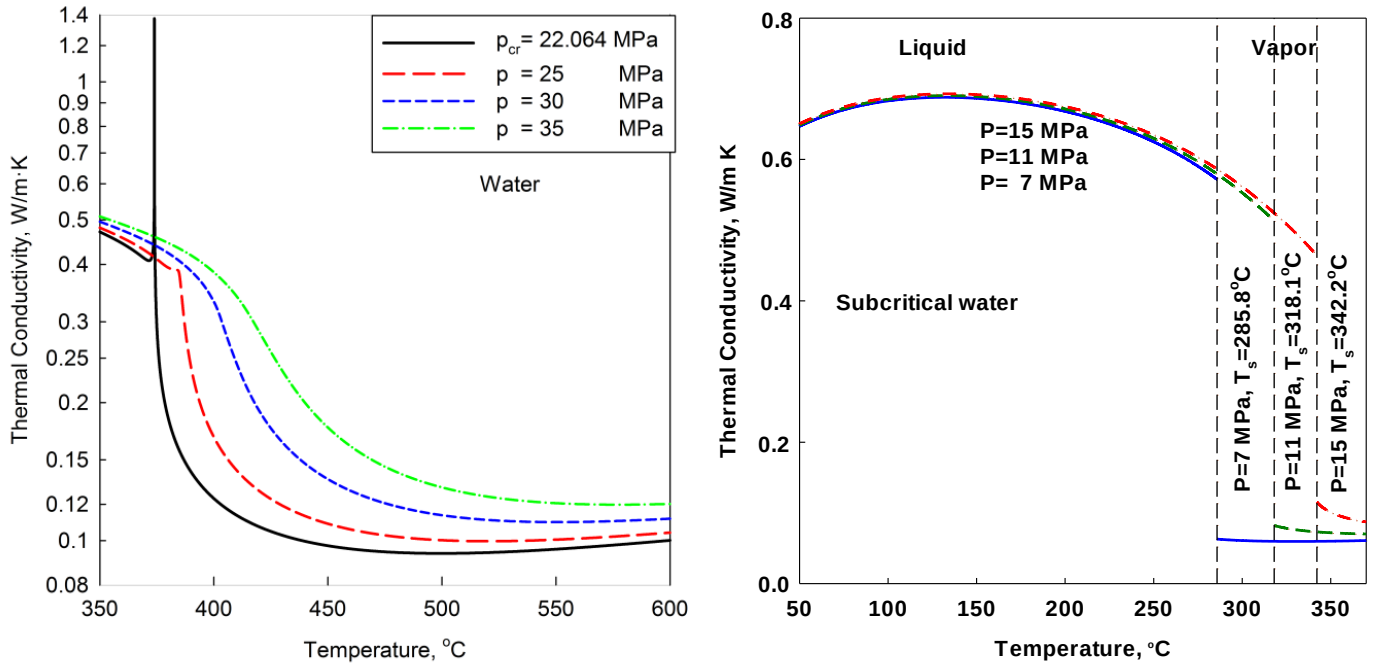

(a) **(b)**

Figure 8a. Thermal conductivity vs. Temperature: Water (a) Critical and supercritical pressures and (b) subcritical pressures.

In general, at least three major approaches can be used for estimation of the characteristic temperature: 1) bulk-fluid temperature approach; 2) wall-temperature approach and 3) film-temperature approach ($T_{film}=(T_w+T_b)/2$). Our studies of forced-convection HT in bare circular tubes with upward flow of SCW (Mokry et al., 2011) showed that the most accurate correlation is based on the bulk-fluid temperature approach:

$$\mathbf{Nu}_b = 0.0061\,\mathbf{Re}_b^{0.904}\overline{\mathbf{Pr}}_b^{0.684}\left(\frac{\rho_w}{\rho_b}\right)^{0.564}, \quad (1)$$

Equation (1) has an uncertainty of ±25% for HTC values and about ±15% for calculated wall temperatures and is valid within the following range: Pressures 22.8-29.4 MPa, heat fluxes 70-1250 kW/m^2, mass fluxes 200-1500 kg/m^{2}s, and tube inside diameters 3-28 mm. Also, it should be noted that this correlation is only for NHT and IHT regimes. Moreover, an independent study by a team of researchers from the University of Ottawa showed that Equation (1) is the most accurate compared to other 16 SCW correlations (Zahlan et al., 2011, 2010) and also, is the most accurate for superheated-steam data.

However, Equation (1) has significantly less accuracy in generalizing data for SC CO_2 flowing upward in vertical bare circular tubes (Gupta et al., 2013). Therefore, a new correlation based on the wall-temperature approach was developed within these conditions:

$$\mathbf{Nu_w} = 0.0038\,\mathbf{Re_w}^{0.957}\,\overline{\mathbf{Pr_w}}^{-0.14}\left(\frac{\rho_w}{\rho_b}\right)^{0.84}\left(\frac{k_w}{k_b}\right)^{-0.75}\left(\frac{\mu_w}{\mu_b}\right)^{-0.22} \quad (2)$$

Equation (2) has an uncertainty of ±30% for HTC values and about ±20% for calculated wall temperatures and is valid within the following range: Pressures 7.6 - 8.8 MPa, heat fluxes 9.3 - 617 kW/m^2, mass fluxes 706 - 3170 kg/m^{2}s, and tube inside diameter of 8 mm. Also, it should be noted that this correlation is also only for NHT and IHT regimes.

However, in SCWRs a bundle flow geometry will be used instead of circular tubes. Therefore, we need to be sure that specifics of HT in circular tubes such as NHT, IHT and DHT regimes are also applicable to the bundle flow geometry. In previous publications (IAEA, 2014; Pioro and Duffey, 2007) it was assumed that HTCs in circular bare tubes will be lower than those in bundle geometry due to HT enhancement with bundle endplates, baring pads, spacers, grids, etc. Therefore, HT correlations obtained in circular bare tubes (e.g., Eq. (1)) can be used as a conservative, but still a preliminary approach in calculations of forced-convective HT in bundle geometry.

In support of this assumption experiments have been performed in an annular channel with a heated rod (see Figs. 9, 11, and 12-14); in a 3-rod bundle (see Figs. 10, 11, 15-17); and in 7-rod bundle (see Figs. 18 and 19) cooled with SCW. These figures are based on Razumovskiy et al. (2015) for annulus and 3-rod bundle; and on Razumovskiy et al. (2013). Uncertainties of measured and calculated parameters are also listed in these two publications.

Analysis of data presented in Figs. 12-14 for the annular channel; in Figs. 15-17 for 3-rod bundle and in Fig. 19 – for 7-rod bundle; shows that depends of operating conditions all three HT regimes can be found. Comparison of HTCs calculated through Eq. (1) (i.e., for circular bare tube) with those of NHT and IHT regimes in the annular channel and 3-rod bundle shows that HTCs in circular flow geometry are lower than in other flow geometries.

Therefore, accounting on a wide variety of possible bundle designs and significant difficulties in testing bundle flow geometries it is reasonable to use circular-bare-tube HT correlations as a conservative approach to estimate HTCs in bundle geometries.

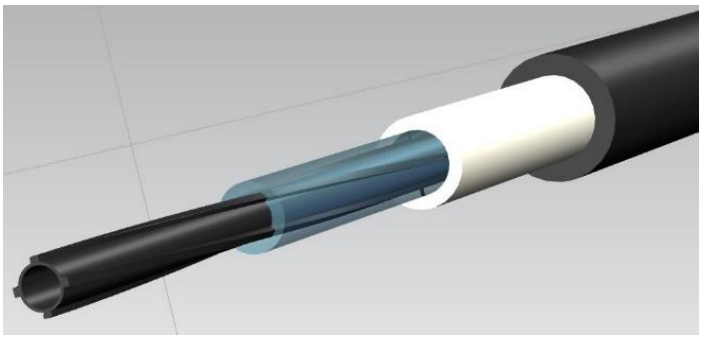

Figure 9. 3-D image of heated-central-rod annular channel.

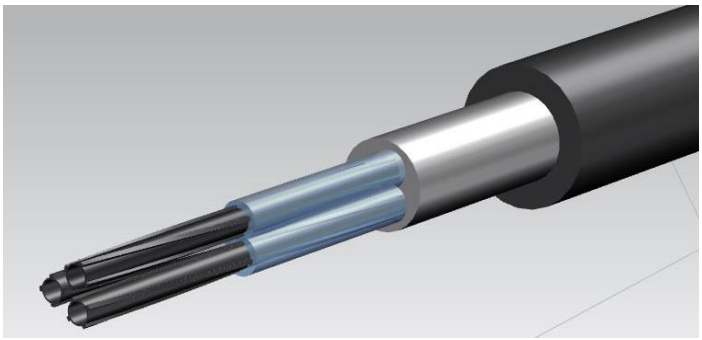

Figure 10. 3-D image of 3-rod bundle.

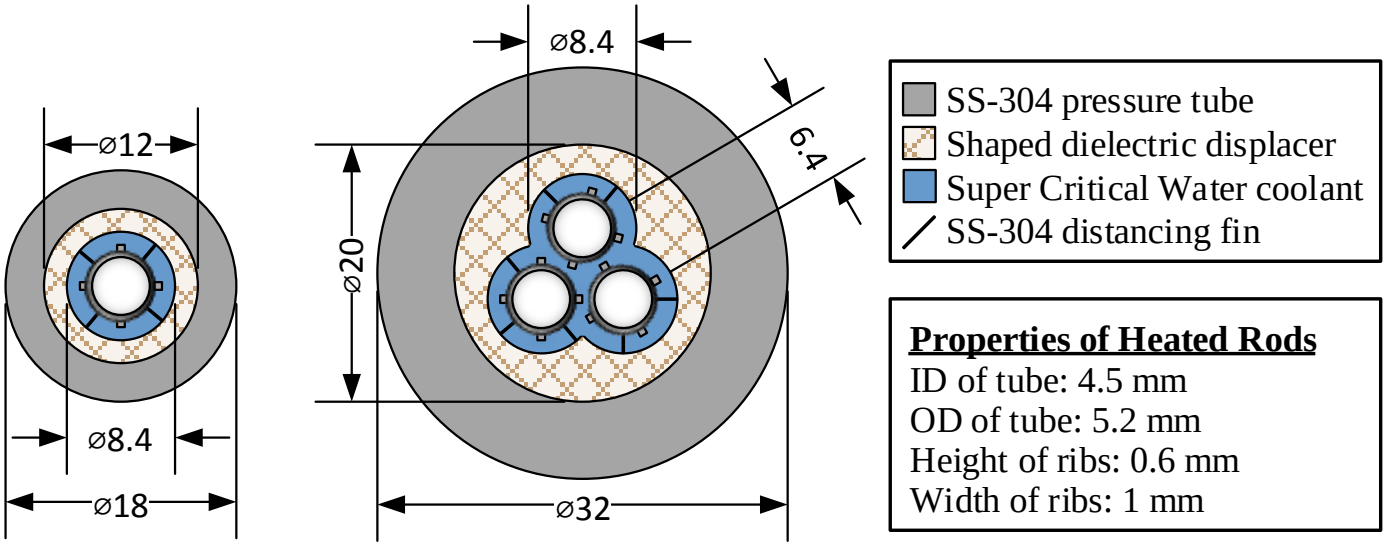

Figure 11. Radial cross-sections of annular channel and 3-rod bundle (note: actually, a Ukrainian stainless steel has been used, but by content and other parameters this steel is very close to SS-304).

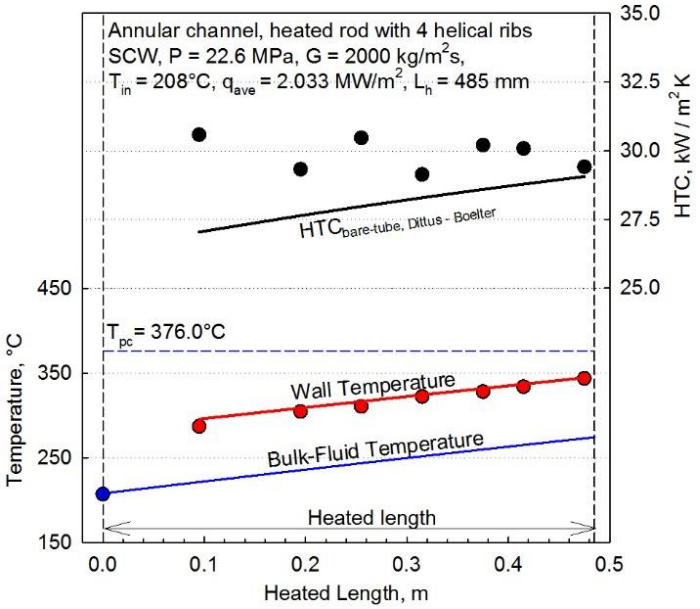

Figure 12. Bulk-fluid-temperature, wall-temperature and HTC profiles along heated length of annular channel: Symbols – experimental data; Lines – calculated profiles; Heat flux - 2.033 MW/m^2.

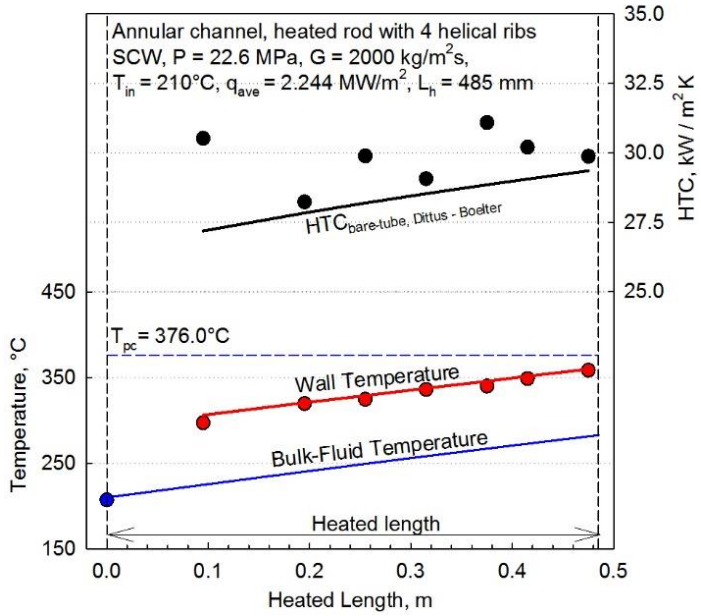

Figure 13. Bulk-fluid-temperature, wall-temperature and HTC profiles along heated length of annular channel: Symbols – experimental data; Lines – calculated profiles; Heat flux - 2.244 MW/m^2.

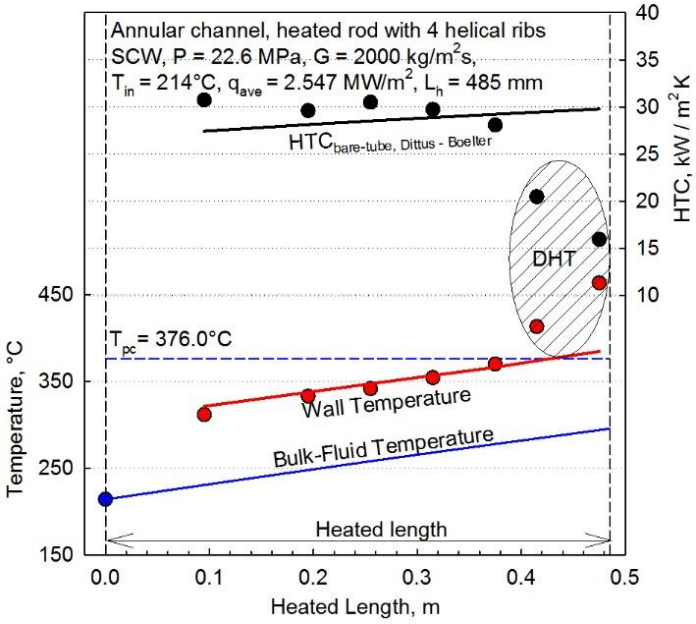

Figure 14. Bulk-fluid-temperature, wall-temperature and HTC profiles along heated length of annular channel: Symbols – experimental data; Heat flux - 2.547 MW/m^2.

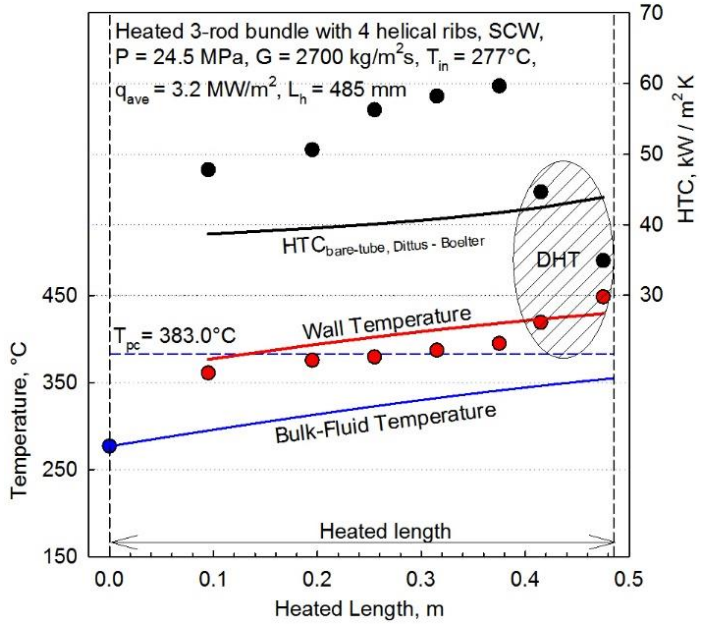

Figure 15. Bulk-fluid-temperature, wall-temperature and HTC profiles along heated length of 3-rod bundle: Symbols – experimental data; Heat flux - 3.2 MW/m^2.

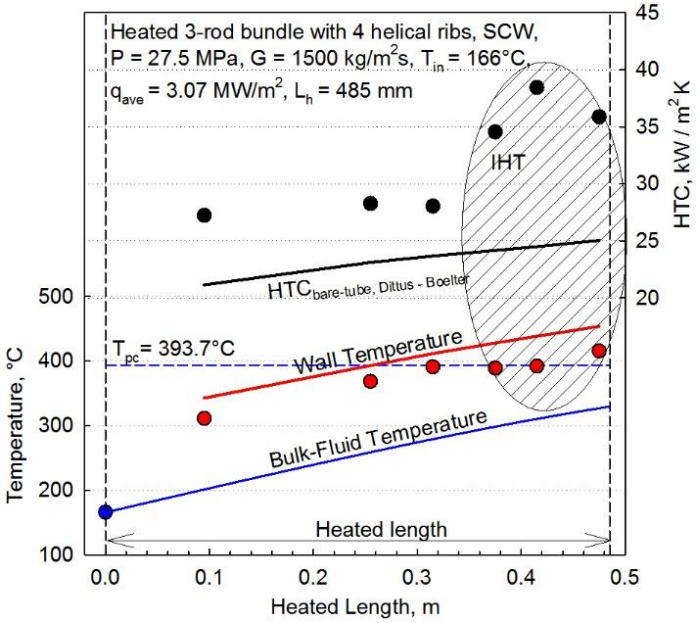

Figure 16. Bulk-fluid-temperature, wall-temperature and HTC profiles along heated length of 3-rod bundle: Heat flux - 3.070 MW/m^2 and inlet temperature - 166°C.

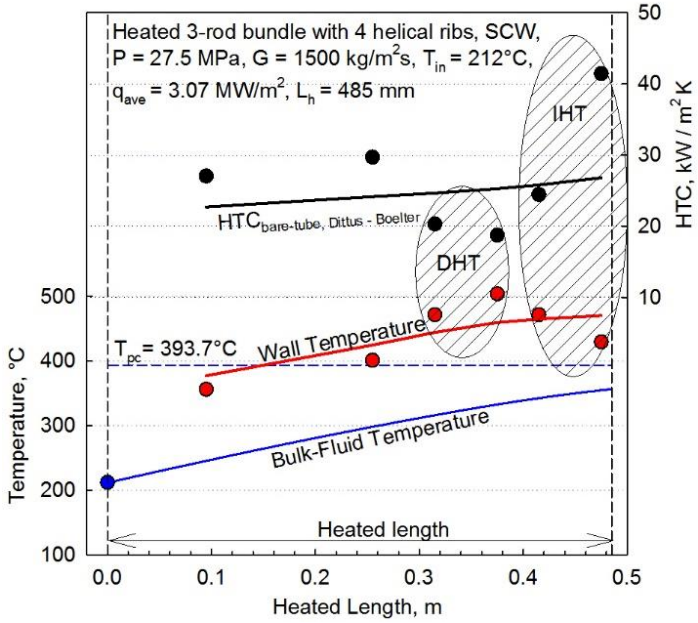

Figure 17. Bulk-fluid-temperature, wall-temperature and HTC profiles along heated length of 3-rod bundle: Heat flux - 3.070 MW/m^2 and inlet temperature - 212°C.

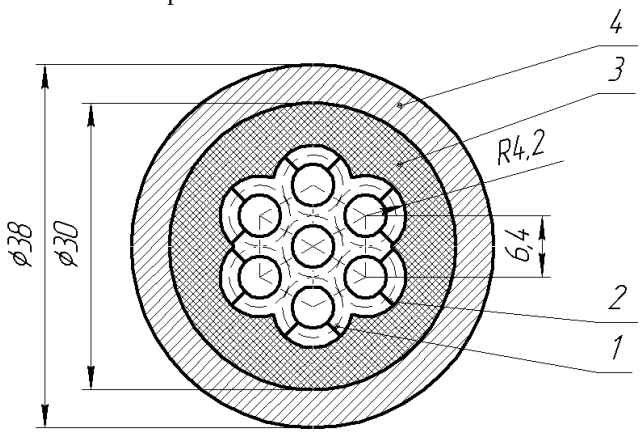

Figure 18. Cross-section of 7-rod bundle: 1 – heated rod; 2 – distancing rib; 3 – shaped dielectric displacer; 4- pressure tube.

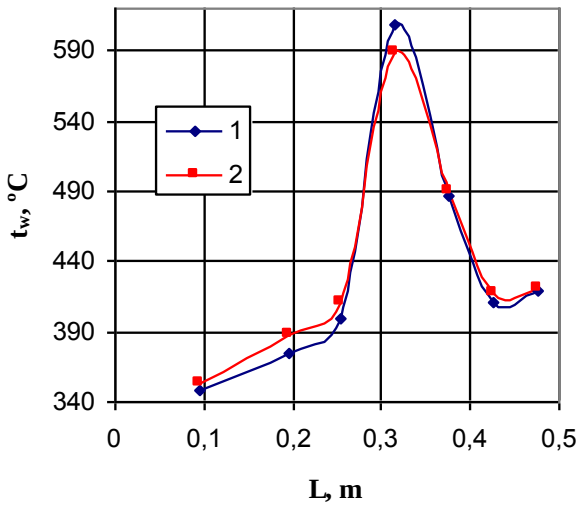

Figure 19. Dependence of deteriorated temperature profile upon water pressure in 7-rod bundle: P, MPa: 1 – 22.6; 2 – 27.5.

CONCLUSIONS

1. Supercritical fluids are used quite intensively in various industries. The application of SCW/"steam" in the power industry has significantly increased the thermal efficiency of power plants. Based on this experience, the next-generation of NPPs will use SCF power cycles such as the Rankine SC "steam" cycle and the SC carbon-dioxide Brayton gas-turbine cycle.
2. Several heat-transfer correlations have been developed for SCW flowing upward in vertical bare tubes. The correlation based on the bulk-fluid-temperature approach appeared to be the most accurate one compared to other 16 correlations. This correlation has an uncertainty of ±25% for HTC values and about ±15% for calculated wall temperatures and is valid within the following range: Pressures 22.8 − 29.4 MPa, heat fluxes 70 − 1250 kW/m^2, mass fluxes 200 − 1500 kg/m^{2}s, and tube inside diameters 3 − 28 mm.

3. However, the developed SCW correlation has less accuracy when applied to SC carbon-dioxide data. Therefore, a new correlation based on the wall-temperature approach was developed. This correlation has an uncertainty of ±30% for HTC values and about ±20% for calculated wall temperatures and is valid within the following range: Pressures 7.6 - 8.8 MPa, heat fluxes 9.3 - 617 kW/m^2, mass fluxes 706 - 3170 kg/m^{2}s, and tube inside diameter 8 mm.
4. Experimental data obtained in annular channel, 3- and 7-rod bundle flow geometries showed that: (a) all three HT regimes: 1) NHT; 2) IHT; and 3) DHT; can be found in these flow geometries; (b) HTCs in circular bare tubes are lower than those in the abovementioned flow geometries; therefore, it is reasonable to use circular-bare-tube HT correlations as a conservative approach to estimate HTCs in bundle geometries.

REFERENCES

Dragunov, A., Saltanov, Eu., Pioro, I., Kirillov, P., and Duffey, R., 2015. Power Cycles of Generation III and III$^+$ Nuclear Power Plants, ASME Journal of Nuclear Engineering and Radiation Science, Vol. 1, No. 2, 10 pages.

Dragunov, A., Saltanov, Eu., Pioro, I., Kirillov, P., and Duffey, R., 2014. Power Cycles of Generation III and III+ Nuclear Power Plants, Proceedings of the 22nd International Conference On Nuclear Engineering (ICONE-22), July 7-11, Prague, Czech Republic, Paper #30151, 13 pages.

Gupta, S., Saltanov, Eu., Mokry, S., Pioro, I., Trevani, L. and McGillivray, D., 2013. Developing Empirical Heat-Transfer Correlations for Supercritical CO_2 Flowing in Vertical Bare Tubes, Nuclear Engineering and Design, Vol. 261, pp. 116-131.

Handbook of Generation IV Nuclear Reactors, 2016. Editor: I.L. Pioro, Elsevier, New York, NY, USA, 938 pages.

IAEA-TECDOC-1746, 2014. Heat Transfer Behaviour and Thermohydraulics Code Testing for Supercritical Water Cooled Reactors (SCWRs), IAEA TECDOC Series, September, Vienna, Austria, 496 pages. Free download from: http://www-pub.iaea.org/books/IAEABooks/10731/Heat-Transfer-Behaviour-and-Thermohydraulics-Code-Testing-for-Supercritical-Water-Cooled-Reactors-SCWRs.

Levelt Sengers, J.M.H.L., 2000. Supercritical Fluids: Their Properties and Applications, Chapter 1, in book: Supercritical Fluids, editors: E. Kiran et al., NATO Advanced Study Institute on Supercritical Fluids – Fundamentals and Application, NATO Science Series, Series E, Applied Sciences, Kluwer Academic Publishers, Netherlands, vol. 366, p. 1.

Mokry, S., Pioro, I.L., Farah, A., King, K., Gupta, S., Peiman, W. and Kirillov, P., 2011. Development of Supercritical Water Heat-Transfer Correlation for Vertical Bare Tubes, Nuclear Engineering and Design, Vol. 241, pp. 1126-1136.

NIST REFPROP, 2010. NIST Standard Reference Database 23: Reference Fluid Thermodynamic and Transport Properties-REFPROP, Lemmon, E.W., Huber, M.L. and McLinden, M.O., Version 9.1, National Institute of Standards and Technology, Standard Reference Data Program, Gaithersburg.

Pioro, I., 2011. The Potential Use of Supercritical Water-Cooling in Nuclear Reactors. Chapter in Nuclear Energy Encyclopedia: Science, Technology, and Applications, Editors: S.B. Krivit, J.H. Lehr and Th.B. Kingery, J. Wiley & Sons, Hoboken, NJ, USA, pp. 309-347.

Pioro, I. and Duffey, R., 2015. Nuclear Power as a Basis for Future Electricity Generation, ASME Journal of Nuclear Engineering and Radiation Science, Vol. 1, No. 1, 19 pages. Free download from: http://nuclearengineering.asmedigitalcollection.asme.org/article.aspx?articleID=2085849.

Pioro, I.L. and Duffey, R.B., 2007. Heat Transfer and Hydraulic Resistance at Supercritical Pressures in Power Engineering Applications, ASME Press, New York, NY, USA, 334 pages.

Pioro, I. and Kirillov, P., 2013a. Current Status of Electricity Generation at Thermal Power Plants, Chapter in the book: Materials and Processes for Energy: Communicating Current Research and Technological Developments, Energy Book Series #1, Editor: A. Méndez-Vilas, Publisher: Formatex Research Center, Spain, Free download from: http://www.formatex.info/energymaterialsbook/book/

Pioro, I. and Kirillov, P., 2013b. Current Status of Electricity Generation at Nuclear Power Plants, Chapter in the book: Materials and Processes for Energy: Communicating Current Research and Technological Developments, Energy Book Series #1, Editor: A. Méndez-Vilas, Publisher: Formatex Research Center, Spain, pp. 806-817. Free download from: http://www.formatex.info/energymaterialsbook/book/806-817.pdf.

Pioro, I. and Kirillov, P., 2013c. Generation IV Nuclear Reactors as a Basis for Future Electricity Production in the World, Chapter in the book: Materials and Processes for Energy: Communicating Current Research and Technological Developments, Energy Book Series #1, Editor: A. Méndez-Vilas, Publisher: Formatex Research Center, Spain, pp. 818-830. Free download from: http://www.formatex.info/energymaterialsbook/book/818-830.pdf.

Pioro, I. and Mokry, S., 2011. Thermophysical Properties at Critical and Supercritical Conditions, Chapter in book "Heat Transfer. Theoretical Analysis, Experimental Investigations and Industrial Systems", Editor: A. Belmiloudi, INTECH, Rijeka, Croatia, pp. 573-592. Free download from: http://www.intechopen.com/books/heat-transfer-theoretical-analysis-experimental-investigations-and-industrial-systems/thermophysical-properties-at-critical-and-supercritical-pressures.

Pioro, I. and Mokry, S., 2011. Heat Transfer to Fluids at Supercritical Pressures, Chapter in book "Heat Transfer.

Theoretical Analysis, Experimental Investigations and Industrial Systems", Editor: A. Belmiloudi, INTECH, Rijeka, Croatia, pp. 481-504. Free download from: http://www.intechopen.com/books/heat-transfer-theoretical-analysis-experimental-investigations-and-industrial-systems/heat-transfer-to-supercritical-fluids.

Pioro, I., Mokry, S. and Draper, Sh., 2011. Specifics of Thermophysical Properties and Forced-Convective Heat Transfer at Critical and Supercritical Pressures, Reviews in Chemical Engineering, Vol. 27, Issue 3-4, pp. 191–214.

Razumovskiy, V.G., Pis'mennyi, Eu.N., Sidawi, K., Pioro, I.L., Maevskiy, E.M., and Koloskov, A.Eu., 2015. Specifics of Heat Transfer to Supercritical Water Flowing Upward in Annular Channel and 3-Rod Bundle, Proc. of the 7th International Symposium on Supercritical Water-Cooled Reactors (ISSCWR-7), March 15-18, Helsinki, Finland, Paper #2095, 11 pages.

Razumovskiy, V.G., Mayevskiy, E.M., Koloskov, A.E., Pis'mennyi, E.N. and Pioro, I.L., 2013. Heat Transfer to Water at Supercritical Parameters in Vertical Tubes, Annular Channels, 3- and 7-Rod Bundles, Proceedings of the 21st International Conference on Nuclear Engineering (ICONE-21), July 29-August 2, Chengdu, China, Paper #16442, 8 pages.

Schmidt, E., Eckert, E. and Grigull, V., 1946. Heat Transfer by Liquids near the Critical State, AFF Translation, No. 527, Air Materials Command, Wright Field, Dayton, OH, USA, April.

Zahlan, H., Groeneveld, D.C., Tavoularis, S., Mokry, S. and Pioro, I., 2011. Assessment of Supercritical Heat Transfer Prediction Methods, Proc. 5th Int. Symp. on SCWR (ISSCWR-5), Vancouver, BC, Canada, March 13-16, Paper P008, 20 pages.

Zahlan, H., Groeneveld, D., and Tavoularis, S., 2010. Look-Up Table for Trans-Critical Heat Transfer, Proc. 2nd Canada-China Joint Workshop on Supercritical Water-Cooled Reactors (CCSC-2010), Toronto, Ontario, Canada: Canadian Nuclear Society (CNS), April 25-28.